Respiratory Motion Compensation for C-arm CT Liver Imaging

Aline Sindel[1], Marco Bögel[1,2], Andreas Maier[1,2], Rebecca Fahrig[3], Joachim Hornegger[1,2], Arnd Dörfler[4]

[1]Pattern Recognition Lab, FAU Erlangen-Nürnberg
[2]Erlangen Graduate School in Advanced Optical Technologies (SAOT), FAU Erlangen-Nürnberg
[3]Stanford, Department of Radiology, Stanford University, Palo Alto, CA, USA
[4]Department of Neuroradiology, Universitätsklinikum Erlangen, Erlangen, Germany
aline.sindel@fau.de

Abstract. In C-arm CT 3-D liver imaging, breathing leads to motion artifacts due to the relatively long acquisition time. Often, even with breath-holding residual respiratory motion can be observed. These artifacts manifest in blurring and interfere clinical investigations such as liver tissue imaging. For 3-D medical image reconstruction a respiratory motion estimation and compensation is required. In this work, the motion was estimated by tracking the motion of the diaphragm and of a vessel bifurcation. The motion signals were integrated into a Thin-Plate-Spline that was used for intra-scan motion compensated reconstruction. This approach was applied to clinical C-arm CT data of the liver and showed improved image quality. Reduced artifacts allow a more precise visual depiction of the liver tissue for liver imaging.

1 Introduction

C-arm CT systems have enabled CT-like 3-D imaging in the interventional suite and are heavily used in many fields, e.g. angiography, cardiology, etc. Tissue imaging of the liver supports the diagnosis of liver diseases that are indicated by a disturbed blood flow and supports cancer treatment.

Liver imaging is a challenging task for C-arm CT systems. Due to the relatively long acquisition time of $5 - 10$ seconds, liver motion and deformation is caused by breathing. This leads to artifacts which can be reduced by breath-holding. Often, even with breath-holding residual respiratory motion can be observed. Therefore, a respiratory motion compensation is required [1].

One approach to estimate motion is to use external devices, e.g. respiration belts. However, additional equipment is required and has to be synchronized to the X-ray image acquisition. Another approach is to extract the motion signal directly from the acquired C-arm CT data in a projection-based respiratory motion estimation. A promising approach is using the diaphragm motion, which can be automatically detected [2] and has a high correlation with the respiratory motion [3]. Schäfer et al. did first motion compensated reconstructions for liver

C-arm CT in an animal study [1]. The diaphragm based signal is an assumption of liver motion and fits particularly well for the upper parts of the liver in cranial-caudal direction [4]. In this work, we propose to estimate a more complex motion vector field using the tracked motion of a vessel bifurcation and the diaphragm, in order to get a better motion estimate within the liver.

2 Materials and Methods

In this section, we will discuss two approaches for liver motion estimation and compensation. The main movement direction of the liver is cranial-caudal with around $5-25\,\mathrm{mm}$, but the movement in the other directions is also not negligibly small. The motion in the anterior-posterior direction varies between $1-12\,\mathrm{mm}$ and between $1-3\,\mathrm{mm}$ in the left-right direction [3]. Thus, we consider all three displacement directions for motion compensated reconstruction. First, we estimate the liver motion by tracking a vessel bifurcation and the diaphragm in the projection images. The resulting motion signals are then used in our main approach to interpolate a 4-D motion vector field. The other approach uses a single 3-D motion signal. Our motion compensated reconstruction is a voxel-driven algorithm based on Schäfer et al. [5] and is implemented in the Software Framework CONRAD [6].

2.1 Motion Signal Estimation

For the upper part of the liver, the diaphragm is very suitable as a surrogate because it is clearly identifiable in the projection images and the cranial-caudal movement is well correlated with the liver movement. However, for tissue imaging a compensation of the inner structure is especially necessary. For this purpose, we tracked a vessel bifurcation that is located within the liver throughout the projection image series.

Finally, we use a rectified motion corrected triangulation algorithm to determine a 3-D position for each projection based on motion corrected point correspondences in orthogonal projection image pairs and hence compute the corresponding motion of the 3-D positions. The motion signal consists of the displacements of the triangulated 3-D points with respect to a reference point, e.g. the first 3-D position [2,7].

Diaphragm 3-D Motion Signal We acquire a 3-D motion signal at the diaphragm top by tracking the contour of the diaphragm in the projection images. Therefore, the images are preprocessed by a gaussian low-pass filter and the Canny edge detector. The contour is tracked using a parabolic function $v = au^2 + bu + c$, where u and v are the detector coordinates. Using a triangulation algorithm, a 3-D motion vector is computed [2,7]. A plot of the motion signal is provided in Fig. 1.

Vessel 3-D Motion Signal In order to get an estimate for internal liver motion, we manually tracked a vessel located in the center of the liver. A plot of the resulting motion signal is provided in Fig. 1. For manual tracking we require a distinctive position of the vessel, which is visible in all projections, e.g. slightly above a vessel branching. Due to the elongated shape of a vessel, we obtain precise information about the displacement in the x and y direction.

2.2 Motion Compensation using a rigid Motion Model

For this method we assume that all parts of the liver are moving in the same direction and in the same speed. With this limitation we can describe the motion of the liver between the projections by only one 3-D motion signal. Furthermore, we will not deal with compression or deformation of the liver in this method, but we assume a uniform voxel shift.

Our motion compensated reconstruction is based on Schäfer et al., in which all voxels are shifted corresponding to their current motion signal, i.e. during the backrojection process the value of the detector pixel corresponding to the shifted voxel is backprojected to the original voxel [5].

Since we refer to only one motion signal in this reconstruction method, we have a constant shift of all voxels for each projection, but the scale and direction of the shift depends on each individual projection. We use the vessel 3-D motion signal to determine the displacement between the projections. As an internal part of the liver, the vessel represents the liver motion and is best suitable for this approach.

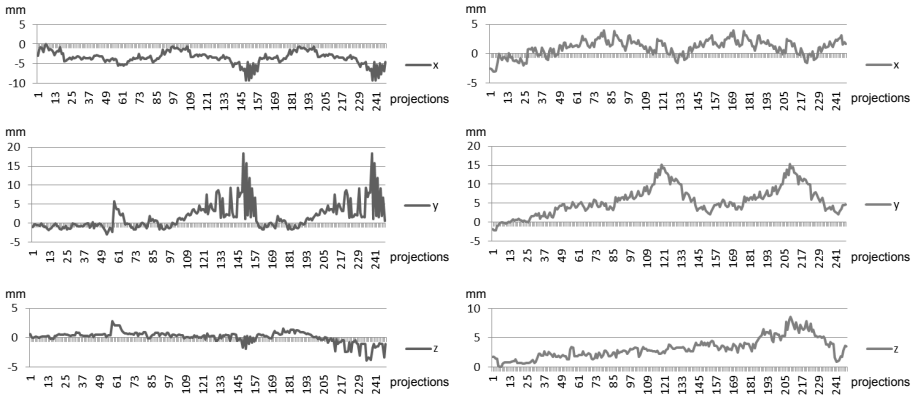

(a) diaphragm motion (b) vessel bifurcation motion

Fig. 1. Comparison of 3-D motion signals: a) diaphragm motion, b) vessel bifurcation motion.

2.3 Motion Compensation using a non-rigid Motion Model

In this method we assume a more complex motion model. We expect a stronger motion in the upper parts because these parts are directly affected by breathing and a decline of motion amplitude in z-direction towards the liver bottom. In order to estimate such a non-rigid motion we use a 4-D motion vector field. Therefore, we build a series of 3-D Thin-Plate-Spline (TPS) consisting of the following control points: (i) 3-D diaphragm signal, (ii) 3-D vessel signal, (iii) boundary points. In this case boundary points refer to points located outside of the volume where we set motion to zero. Thus, the TPS algorithm is more flexible to handle rigid objects as ribs and spine.

For each projection we create a 3-D motion vector field that consists of the displacement vectors determined by the TPS Interpolation. The displacement vector $\mathbf{d}(\mathbf{x})$ of an arbitrary voxel $\mathbf{x} \in \mathbb{R}^3$ is defined as

$$\mathbf{d}(\mathbf{x}) = \mathbf{A}\mathbf{x} + \mathbf{b} + \sum_{i=1}^{n} \mathbf{G}(\mathbf{x} - \mathbf{p}_i)\mathbf{c}_i \tag{1}$$

where $\mathbf{p}_i$ are the control points and $\mathbf{G}$ is the transformation's kernel matrix to measure the euclidean distance to the control points, with the weighting coefficients $\mathbf{c}_i$. $\mathbf{A} \in \mathbb{R}^{3\times3}$ and $\mathbf{b} \in \mathbb{R}^3$ specify an additional affine transformation to regulate higher deviations of the spline to the control points [8]. The control points are set for each motion vector field estimation depending on the projection specific motion signals.

We use a voxel-based motion compensated backprojection as described above for the reconstruction, but in this case the voxels are shifted according to their motion vector field entries. The TPS-coefficients are estimated prior to reconstruction. The TPS is then evaluated during the backprojection on the GPU.

3 Results

We used clinical data to evaluate our motion compensation methods. The projection data was acquired for liver imaging using a C-arm CT system with administration of contrast agent and as native scans. One acquisition consisted of 248 projections with 640×480 pixels and a resolution of $0.616\ \frac{\text{mm}}{\text{pixel}}$. The motion compensated reconstructions have been compared to a standard FDK reconstruction of the same projection data. An example of the result images is shown in Fig. 2.

The uncompensated reconstructions showed several motion artifacts (Fig. 2a). The whole liver tissue was blurred. This was obvious to see at the vessels in the axial view, where the vessels were half circle shaped instead of point-shaped. The liver borders and the diaphragm showed doubling and distortion.

The first method for motion compensated reconstruction (rigid motion model) indicated a great improvement (Fig. 2b). Using a single 3-D motion signal of a vessel bifurcation located in the liver center, the liver tissue appeared sharper

and the vessels were mapped point-like. However, there was some blurring at the upper border of the liver.

The second motion compensated reconstruction method (non-rigid motion model) combined the 3-D motion signals of diaphragm and vessel in a TPS. These reconstructions further reduced motion artifacts (Fig. 2c). Additionally, they offered considerably higher image quality at the liver top and in the surrounding tissue. The vessel contour was more distinct with less streak artifacts in contrast to the first method.

We evaluated the image quality of the different reconstruction results by a survey with four experts that have scored the images on a scale from 1 to 5 (best: 5). We used four different slices of a contrast injected scan and four of a scan with residual contrast agent. The results are given as mean ± standard deviation. The compensated reconstruction images had a higher score (3.6 ± 0.51

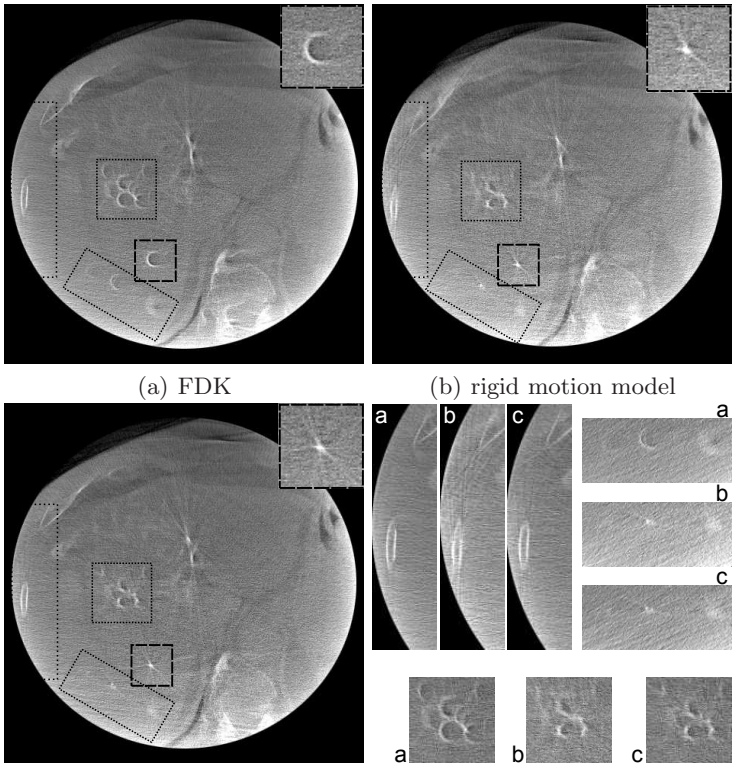

(a) FDK (b) rigid motion model

(c) non-rigid motion model (d) ROIs

Fig. 2. Comparison of uncompensated and motion compensated reconstruction (with contrast agent): a) uncompensated reconstruction (FDK), b) motion compensated reconstruction using a vessel 3-D signal, c) motion compensated reconstruction using a 4-D motion vector field. An enlarged version of the tracked vessel is to see in the top right corner. d) These ROIs highlight the vessels in the surroundings and the ribs.

for TPS and 3.2 ± 0.54 for one signal compensation) than the uncompensated ones (1.1 ± 0.18). In total the TPS compensation was valued best, in 6 out of 8 cases it scored better than the compensation with a single signal.

4 Discussion

We presented an algorithm to compensate respiratory motion in C-arm CT liver imaging. As shown in the result section, we observed a great improvement in image quality for liver tissue images using the motion compensated reconstruction methods. We were able to handle the artifact of distorted vessels and achieved a sharper liver border. The motion compensated reconstruction methods enable the visualization of small structures in liver tissue. We observed good results using a single tracked vessel and the diaphragm top. However, the TPS is a more flexible algorithm. More than one vessel could be used as control points and a segmented surface of the liver could contribute further control points to the TPS. For successful motion compensation it is important that the diaphragm top is visible completely in all scans and that a vessel bifurcation or an other feature is detectable in all images. So far, the vessel tracking was done manually. Future work will be looking into automatic tracking of image features in the projection images.

References

1. Schäfer D, Lin M, Rao PP, Liapi E, Noordhoek N, Eshuis P, et al. Breathing motion compensated reconstruction for C-arm cone beam CT imaging: initial experience based on animal data. In: Medical Imaging 2012: Physics of Medical Imaging. vol. 8313. San Diego, California, USA: Proc. SPIE; 2012. p. 83131D–83131D–6.
2. Bögel M, Hofmann HG, Hornegger J, Fahrig R, Britzen S, Maier A. Respiratory Motion Compensation Using Diaphragm Tracking for Cone-Beam C-Arm CT: A Simulation and a Phantom Study. Int J Biomed Imaging. 2013;2013(1):1–10.
3. von Siebenthal M. Analysis and Modelling of Respiratory Liver Motion using 4DMRI [PhdThesis]. ETH Zurich; 2008.
4. Balter JM, Dawson LA, Kazanjian S, et al. Determination of ventilatory liver movement via radiogrphic evaluation of diaphragm position. Int J Radiation Oncology Biol Phys. 2001;51(1):267–270.
5. Schäfer D, Borgert J, Rasche V, Grass M. Motion-Compensated and Gated Cone Beam Filtered Back-Projection for 3-D Rotational X-Ray Angiography. IEEE Trans Med Imaging. 2006;25(7):898–906.
6. Maier A, Hofmann HG, Berger M, Fischer P, Schwemmer C, Wu H, et al. CONRAD-A software framework for cone-beam imaging in radiology. Med Phys. 2013;40(11):111914–1–111914–8.
7. Bögel M, Riess C, Maier A, Hornegger J, Fahrig R. Respiratory Motion Estimation using a 3D Diaphragm Model. Proc BVM. 2014; p. 240–245.
8. Müller K, Zheng Y, Lauritsch G, et al. Evaluation of Interpolation Methods for Motion Compensated Tomographic Reconstruction for Cardiac Angiographic C-arm Data. In: Proceedings of the second international conference on image formation in x-ray computed tomography. Salt Lake City, Utah, USA; 2012. p. 5–8.